Generalized flux-gradient technique pairing line-average concentrations on vertically separated paths

J.D. Wilson*, T.K. Flesch

Department of Earth and Atmospheric Sciences, University of Alberta, Edmonton, Canada

ABSTRACT

Line-averaging optical gas detectors offer new avenues for the indirect estimation of surface/air exchange fluxes. This paper examines an inverse dispersion technique (gFG, for "generalized flux-gradient") that yields an estimate of the gas emission rate Q from surface area sources, based on the difference ΔC between line-averaged mean concentrations along two (or more) paths that are vertically inclined or, if horizontal, are vertically separated. The inversion to extract Q from ΔC can be performed using any satisfactory model of turbulent dispersion over a finite source, motivating the examination here of several analytical solutions to the advection-diffusion equation. Each provides a theoretical value $u_* \Delta C/Q$ for the normalized concentration difference, whence an estimate $\widetilde{Q}$ of the flux can be deduced from measured ΔC and u_* (the latter being the friction velocity, for which any suitable velocity scale could be substituted). Discrepancies between the solutions are explored, and the error that results from wrongly treating the source fetch as infinite is quantified. As the fetch increases, gFG relaxes to the standard flux-gradient technique exploiting the (known) Monin–Obukhov concentration gradient.

© 2016 The Authors. Published by Elsevier B.V. This is an open access article under the CC BY license (http://creativecommons.org/licenses/by/4.0/).

1. Introduction

This paper outlines an experimental method for determination of surface-air exchange fluxes "Q" by inverse dispersion, exploiting the flexibility of recently developed line-averaging, open-path optical gas detectors. The technique, which for convenience we label gFG (for "generalized flux-gradient"), is related to the flux-gradient method in that it exploits a vertical difference $(C_1 - C_2)$ in the mean concentration of the gas of interest. However whereas a standard flux-gradient approach derives Q from vertically-separated *point* sensors exposed within a constant flux layer, gFG is based on line-averaged concentrations (along paths, furthermore, that are not necessarily parallel), and it applies even over a limited (but known) fetch of source. Inverse dispersion on the micro-meteorological scale has to date more typically been based on *horizontally*-separated concentration measurements (see survey of Wilson et al., 2012), and in that configuration cannot easily deal with sources of large areal extent or uncertain perimeter.

Suppose the atmospheric surface layer (ASL) is horizontally homogeneous, thus characterized by the friction velocity u_*, Obukhov length L, surface roughness length z_0 and mean wind direction (a single sonic anemometer-thermometer provides

information allowing to deduce these quantities). We will align the horizontal coordinate x with the direction of the mean wind and, with the purpose of illustrating gFG in an idealized source geometry, consider a uniform ground-level source of trace gas lying at $x \geq 0$ and extending to infinity along the crosswind (y) axis. Now consider a pair of gas detector paths that originate at $(x_{e1}, 0, z_{e1})$, $(x_{e2}, 0, z_{e2})$, the "emitter" locations, and whose endpoints (the "reflectors") lie respectively at $(x_{e1} + D_{x1}, 0, z_{r1})$ and $(x_{e2} + D_{x2}, 0, z_{r2})$: Fig. 1 shows a case of special interest, where both paths share a common emitter/detector point (x_c, z_c) and lie in the vertical plane at $y = 0$ (this is an eminently practical configuration, as it represents the case of a fixed optical emitter/detector being sequentially aimed to high and low reflectors). We also accommodate the possibility that the emitter point(s) x_e could lie upwind from the leading edge of the source, a configuration that might be chosen if (for example) the source area were a pond, or ground inhospitable to the placement of instruments, or a herd of animals confined within a paddock.

At the end of a measurement interval the instrument provides time-space mean concentrations C_1, C_2 for the lower and upper paths.[1] Assuming that "background" (or upwind) concentration is spatially and temporally uniform on the scale of interest, the

---

* Corresponding author.
  E-mail address: jaydee.uu@ualberta.ca (J.D. Wilson).

[1] It would be ideal if the instrument were inherently differential – an ideal that some modern detectors almost (though not quite) attain; in the case of the instrument described in the companion paper (Flesch et al., 2016) *almost*, because the
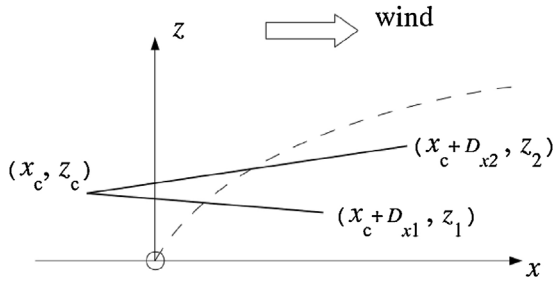
Fig. 1. Schematic of a measurement setup for source estimation by inverse dispersion using a gFG (generalized flux-gradient) method. The upwind edge of the gas source is at the origin ($x = 0$). The equipment returns the time- and line-averaged gas concentrations C_1 and C_2 along respectively the lower and upper grey lines, in this case shown as slant paths with a common emitter/detector position (x_c, z_c). In practice one would prefer that the detection paths lie within the growing gas plume (whose envelope is indicated by the dashed line). For results shown in this paper the two measurement paths have the same projection onto the horizontal axis, i.e. $D_{x1} = D_{x2}$.

difference $\Delta C \equiv (C_1 - C_2)$ is indifferent to its value (C_0). Then if one has a theoretical value $\Phi = u_* \Delta C/Q$ for the "conversion number" relating the unknown source strength Q to the concentration difference, measured u_* and ΔC give an estimate

$$Q_{gFG} = \frac{[u_* \, \Delta C]^{meas}}{\Phi} \tag{1}$$

of the emission rate.

The next section will briefly review available analytical prescriptions for the field of normalized concentration difference $u_* \Delta C/Q$, including solutions of the advection-diffusion equation. In a related paper (Flesch et al., 2016) gFG is performed on the basis of a more advanced Lagrangian stochastic (LS) trajectory model, however the purpose here is to look at the technique more broadly, evaluating a practicable technique that does not carry the computational burden inherent in computing turbulent trajectories: for doing so necessitates a time consuming computation of backward-time trajectories from representative points all along the (slanted) detector paths. In such a context the ~10% level of accuracy is about what one might realistically hope for, certainly for individual inversions (i.e. circa 15–30 min averaging intervals): averaging over repeated trials should narrow that uncertainty.

2. Formulae for the conversion: $u_* \, \Delta C \longrightarrow Q$

Stationarity of both the micrometeorological state and of the tracer field is assumed, and the following notation is used: $\bar{c} = \bar{c}(x, y, z)$ represents the mean concentration at a single point, while C will designate an average value of $\bar{c}$ along a measurement path, i.e C is a shorthand notation for $\langle \bar{c} \rangle$, with $\langle \rangle$ designating the line-averaging operation.

2.1. Inversion using the MO concentration profile (infinite fetch implied)

Two estimates of the conversion number $\Phi \equiv u_* \Delta C/Q$, both *neglecting edge effects*, can be extracted from the Monin–Obukhov concentration profile, i.e.

$$\bar{c}^{MO}(z) = \bar{c}^{MO}(z_0) + \frac{C_*}{k_v/S_c} \left[\ln \frac{z}{z_0} - \psi_c \left(\frac{z}{L} \right) + \psi_c \left(\frac{z_0}{L} \right) \right] \tag{2}$$

where C_* ($\equiv -Q/u_*$) is the tracer concentration scale, k_v (=0.4) is the von Karman constant, and S_c (Schmidt number) is the ratio of

the eddy viscosity to the eddy diffusivity in the neutral limit. The diabatic correction function ψ_c is here evaluated as

$$\psi_c = \psi_c(\phi_c) = 2 \ln \left[\frac{1}{2} \left(1 + \phi_c^{-1} \right) \right], \tag{3}$$

with ϕ_c given by (Dyer and Hicks, 1970)

$$\phi_c = 1 + 5z/L, \quad L \geq 0, \tag{4}$$

$$\phi_c = (1 - 16z/L)^{-1/2}, \quad L < 0. \tag{5}$$

Eq. (2) can be applied to compute the difference in the line averaged concentrations ("Φ_{MO}") or the difference between the concentrations at the *midpoints* of the two beams ("Φ_{MO-mid}"): if the MO concentration profile were linear with height, these would coincide. For the MO solutions, the absolute location of the measurement system relative to the edge of the source has no impact on the conversion number $u_* \Delta C/Q$.

2.2. Formulae that account for limited fetch of source

We neglect variation of wind direction with height, and (as already noted) assume sources extend to infinity in the y direction. All existing formulae for surface layer dispersion are solutions, exact or otherwise, of an advection-diffusion equation (ADE), here[2]

$$\bar{u} \, \frac{\partial \bar{c}}{\partial x} = \frac{\partial}{\partial z} \left[K_c \, \frac{\partial \bar{c}}{\partial z} \right], \tag{6}$$

where $\bar{u} = \bar{u}(z)$ is the mean wind profile and $K_c = K_c(z)$ is the profile of the eddy diffusivity for the species "c". The flow being (by assumption) horizontally homogeneous, the proper (Monin–Obukhov) profiles for insertion in Eq. (6) are

$$\bar{u} = \frac{u_*}{k_v} \left[\ln \frac{z}{z_0} - \psi_m \left(\frac{z}{L} \right) + \psi_m \left(\frac{z_0}{L} \right) \right] \tag{7}$$

and

$$K_c = \frac{(k_v/S_c) u_* z}{\phi_c(z/L)}. \tag{8}$$

The MO function ϕ_c for the concentration profile is given above. The corresponding function ϕ_m for the wind profile was specified as (Dyer, 1974; Dyer and Hicks, 1970)

$$\phi_m = 1 + 5z/L, \quad L \geq 0, \tag{9}$$

$$\phi_m = (1 - 16z/L)^{-1/4}, \quad L < 0, \tag{10}$$

and implies that the diabatic correction function ψ_m in Eq. (7) is

$$\psi_m \left(\frac{z}{L} \right) = -5z/L, \quad L \geq 0, \tag{11}$$

$$\psi_m \left(\frac{z}{L} \right) = 2 \ln \left(\frac{1 + \phi_m^{-1}}{2} \right) + \ln \left(\frac{1 + \phi_m^{-2}}{2} \right)$$
$$- 2 \mathrm{atan} \left(\phi_m^{-1} \right) + \frac{\pi}{2}, \quad L < 0. \tag{12}$$

Exact solutions of Eq. (6) can be obtained if, in lieu of Eqs. (7) and (8), the profiles of wind speed and diffusivity are parameterized as power laws,

$$\bar{u} = \bar{u}_H (z/H_u)^m = \mathcal{U} z^m, \tag{13}$$

$$K_c = K_{cH} (z/H_K)^n = \kappa z^n. \tag{14}$$

---

emitter/detector is common to all paths; but *not quite*, because (for instance) measurements on the paired paths are sequential rather than simultaneous.

The parameters $\bar{u}_H$, K_{cH}, m, n are (or can be) chosen to reproduce the mean wind speed and eddy diffusivity, as well as their height gradients, at the reference height(s) H_u, H_K, which we shall henceforth cease to distinguish ($H \equiv H_u \equiv H_K$): this results in

$$m = \frac{\phi_m(H/L)}{k_v \bar{u}_H / u_*}, \tag{15}$$

$$n = 1 - \frac{H}{\phi_c(H/L)}\left[\frac{\partial \phi_c(z/L)}{\partial z}\right]_{z=H}, \tag{16}$$

$$\bar{u}_H = \frac{u_*}{k_v}\left[\ln\frac{H}{z_0} - \psi_m(H/L) + \psi_m(z_0/L)\right], \tag{17}$$

$$K_{cH} = \frac{(k_v/S_c)u_* H}{\phi_c(H/L)}. \tag{18}$$

2.2.1. Exact solution of the ADE for a surface line source

A solution to Eqs. (6), (13), (14) for a surface line source, provided originally by O.F.T. Roberts (Monin and Yaglom, 1977, p661), has been used by numerous authors, including van Ulden (1978) and Kormann and Meixner (2001). Defining $r = 2 + m - n$ and $\mu = (1 + m)/r$, the concentration at (x, z) due to a continuous (crosswind-oriented) line source of unit strength localised at the origin ($x = z = 0$) is (Kormann and Meixner, 2001, Eqs. (12) and (20))

$$\bar{c}(x, z) = \frac{1}{\Gamma(\mu)} \frac{r}{\mathcal{U}} \frac{1}{z^{1+m}} \left(\frac{\zeta}{x}\right)^{\mu} e^{-\zeta/x} \tag{19}$$

where $\Gamma(\mu)$ is the Gamma function (for whose evaluation see Abramowitz and Stegun, 1953) and

$$\zeta(z) = \frac{\mathcal{U}}{r^2 \kappa} z^r \tag{20}$$

is a transformed height. In order to obtain a theoretical value for $(C_1 - C_2)/Q$ from Eq. (19) a double integration is needed. Each point (x, z) on a measurement path is exposed to an *area* source, such that (provided $x > 0$, i.e. the point in question lies downwind of the leading edge of the source) Eq. (19) must be integrated to define the said area source; then secondly, one must sum up the contributions from every point along the beam. These operations have been performed numerically to obtain the conversion number Φ_{KM} (details below).

2.2.2. Exact solution of the ADE for a surface area source

Philip (1959) gave a solution to Eqs. (6), (13), (14)) for an *area* source, valid provided $n \neq 1$ (i.e. neutral stratification is excluded). Computing the conversion number (Φ_P) based on Philip's solution rather than that of the previous section eliminates one integration, though summation along each measurement path remains essential.

As before, define $r = 2 + m - n$ and $\mu = (1 + m)/r$, and let $\beta = r/(1 - n) \equiv 1/(1 - \mu)$. With

$$\eta = \frac{\mathcal{U} z^r}{r^2 \kappa x} (\equiv \zeta/x), \tag{21}$$

Philip's solution for the mean (point) concentration due to a unit area source at the surface covering $x \geq 0$ is

$$\bar{c}(x, \eta) = \frac{1}{(1-n)\Gamma(\mu)\kappa}\left(\frac{r^2 \kappa x}{\mathcal{U}}\right)^{1/\beta} F(\eta, \beta) \tag{22}$$

where

$$F(\eta, \beta) = 1 - \Gamma(\mu)\eta^{1/\beta} + \frac{\eta}{\beta - 1} - \frac{\eta^2}{2!(2\beta - 1)} + \frac{\eta^3}{3!(3\beta - 1)}$$

$$- \frac{\eta^4}{4!(4\beta - 1)} + \cdots \tag{23}$$

Philip's solution is easy to evaluate, but fails to converge if the distance between the observation point (i.e. a point on the detector beam) and the leading edge of the source is too small, which limits its use in practice to detector paths that do not cross that leading edge. For detector paths lying downstream from the leading edge it will be shown below that the conversion number Φ_P from Philip's solution matches Φ_{KM} perfectly, as (in the absence of discretization error due to the extra numeric integration needed for Φ_{KM}) it should.

2.2.3. Approximate solution of the ADE for surface area source

Wilson (1982)[3] used a method suggested by Shwetz (1949) to obtain an approximate series solution to Eq. (6) with Monin–Obukhov profiles. This was restricted to stable or neutral stratification, but has been extended (Wilson, 2015a) to the unstable case – albeit under the compromise of reintroducing the power law wind profile. The conversion number (Φ_W) is computed as follows. On any given vertical (i.e. at any given distance x from the leading edge of the source) one first determines the depth $z_\delta(x)$ of the gas plume, by solving an implicit equation (Wilson, 1982, Eq. (24) or Eq. (24N) for the stable or neutral case, respectively; Wilson, 2015a, Eq. (21) for the unstable case). If at x a measurement path lies above $z_\delta(x)$, no contribution to the line averaged concentration is made; otherwise the contributing concentration is calculated using Wilson (1982, Eq. 21) for the stable case, Wilson (1982, Eq. 21N) for the neutral case or Wilson (2015a, Eq. 22) for the unstable case.

2.3. Numerical integration to obtain path-averaged concentration

Each of the above analytical solutions provides an estimate $\bar{c}(x, z)$ of the mean concentration at any point, the source itself lying at $x \geq 0$. Now, let $z_P = z_P(x)$ for $x_e \leq x \leq x_e + D_x$ define the line-averaging measurement path, whose length (if it is a light path) is $\sqrt{D_x^2 + (z_r - z_c)^2}$. Line averaging of the analytical (and Monin–Obukhov) solutions for point concentration was performed numerically to obtain the corresponding conversion numbers:

$$C \equiv \langle \bar{c} \rangle = \frac{1}{D_x} \int_{x_e}^{x_e + D_x} \bar{c}(x, z_P(x)) \, dx \approx \frac{1}{D_x} \sum_i \bar{c}(x_i, z_P(x_i)) \, \Delta x \tag{24}$$

where $\Delta x = 0.1$ m ($\ll D_x$).

3. Comparison of conversion numbers (Φ) for test problems

For results to be shown the roughness length is $z_0 = 0.01$ m. All solutions have been evaluated with Schmidt number $S_c = 0.64$ (Wilson, 2015a,b), and unless otherwise stated the reference height for power law profiles is $H = 1$ m.

To examine the importance of the location of the common point (i.e. emitter/detector) relative to the leading edge of the source, we begin with the detector configuration of Fig. 1: the two detector paths slant up (or down) from a common point at (x_c, z_c) with $z_c = 1.5$ m to $z_u = 2.5$ m (or $z_d = 0.5$ m). Fig. (2) plots $\Phi \equiv u_* \Delta C/Q$ (the "conversion number") for three stability conditions $z_0/L = (0.001, 0, -0.001)$ and with x_c ranging from -25 m to 100 m, the x-wise span of the beams being $D_x = 50$ m. In terms of the overall pattern, the conversion number is positive because C_1 is from the lower path;

---

[3] Two corrections to the equations given by Wilson (1982) are noted. The product δr on the second line of his Eq. (21) ought (in order to have been consistent with his Eq. (17), and correct) to have been δr; and two small terms arising from an integration constant ("δ_1") had been neglected in the transition from his Eq. (20) to his Eq. (24).
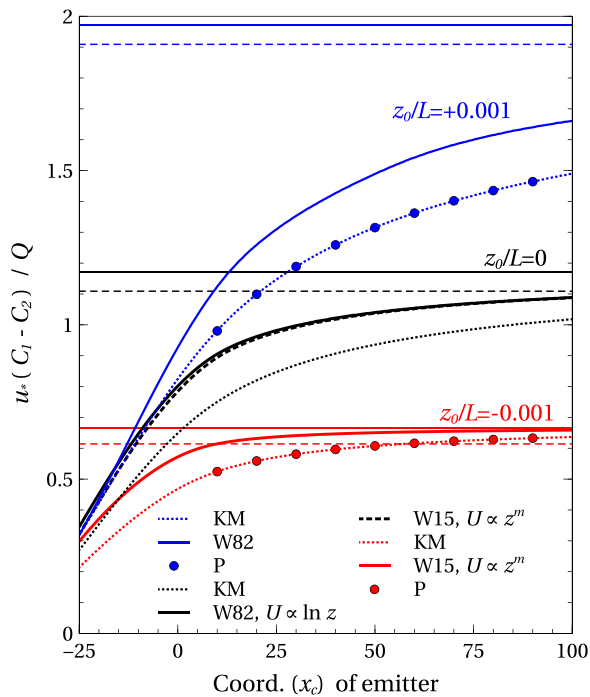
Fig. 2. Estimates for the conversion number $u_* \Delta C/Q$ in the case that the detection paths span $x_c \leq x \leq x_c + 50$ m (i.e. $D_{x1} = D_{x2} = 50$ m), slanting up (or down) from $z_c = 1.5$ m to $z_u = 2.5$ m and $z_d = 0.5$ m, with the emitter/receiver point x_c as much as 25 m upstream or as much as 100 m downstream from the leading edge of the source. Stratification is colour-coded. Legend identifies solutions of Wilson (1982, 2015; W82 or W15), Kormann and Meixner (2001; KM), and (Philip (1959; P). Horizontal lines are the Monin–Obukhov solution, solid where correctly integrated along the paths, and dashed where the concentration difference is taken between the *midpoints* of the beams. The heavy dashed black (neutral) curve is the Wilson (2015a) solution with $\bar{u} \propto z^m$ evaluated for $z_0/L \to 0^-$, while the heavy black solid curve is Wilson (1982) for $z_0/L = 0$ with the log wind profile. Monin–Obukhov solutions neglect the edge effect, and the error in doing so decreases with increasing x_c (i.e. increasing upwind fetch of source).

Fig. 3. As for Fig. 2, but for longer detection paths ($D_x = 100$ m) that span $x_c \leq x \leq x_c + 100$ m, slanting up (or down) from $z_c = 1.5$ m to $z_u = 2.5$ m and $z_d = 0.5$ m. (Philip solution, equivalent to KM, not shown).

and the computed values of $u_* \Delta C/Q$ are larger (smaller) under stable (unstable) stratification than in the neutral case. As expected, the conversion number Φ_P derived from Philip's (1959) area source solution coincides exactly with that (Φ_{KM}) derived (at the cost of an extra integration) from the Kormann and Meixner (2001) point source solution.

In the case of neutral stratification, five distinct solutions for the conversion number are given. The horizontal lines are the conversion numbers that result from neglecting the finite upwind extent of the source (Φ_{MO} and Φ_{MO-mid}). Then (recalling that Philip's solution does not cover the neutral case) it remains to relate the KM solution to the solutions identified as W82 and W15. With $z_0/L = 0$, the Kormann–Meixner (exact) solution and the Wilson (1982) analytic solution share the same eddy diffusivity profile, viz. $K_c = (k_v/S_c)u_* z$ (implying $n = 1$), but they differ in that the former uses a power-law wind profile and the latter the log wind profile. On the evidence of Fig. (2) the two (KM, W82) neutral solutions differ, which raises the question as to whether the difference stems (i) from the differing wind profiles, or (ii) from the loss of accuracy inherent to the (approximate) series solution procedure invoked by Shwetz (1949) and that underlies Wilson (1982, 2015a). The question is easily answered, because the Wilson (2015a) solution (shown with the label "W15, $\bar{u} \propto z^m$" on Fig. 2) had reverted to a power law wind profile and so, in its neutral form, it shares exactly the same profiles as the Kormann–Meixner solution, yet, differs from it. Furthermore the "W82, $\bar{u} \propto \ln z$" and "W15, $\bar{u} \propto z^m$" solutions for $z_0/L = 0$, respectively with the log and power-law wind profile, virtually overlap: hence it is certain that the discrepancy
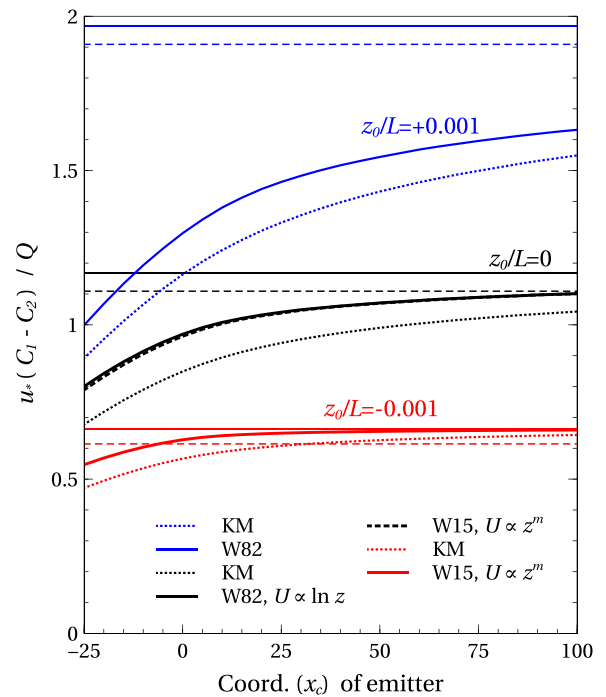
between the Kormann–Meixner solution and W82, W15 is (in the neutral case, at least) due principally to the loss of accuracy inherent in Shwetz's splitting of the advection-diffusion equation (e.g. as exemplified by Eqs. (14) and (15) of Wilson, 2015a), rather than owing to their distinct representations of one or both of the profiles.

Be that as it may, we notice that as the detector beams are shifted far downwind from the leading edge (i.e. as x_c becomes large) the KM (equivalently, P) and W solutions converge – as expected – towards the appropriate Monin–Obukhov solution,[4] (solid horizontal lines, colour coded by stability). However when x_c is *not* large we see that a significant degree of error would be incurred by inverting the measured concentration difference using the Monin–Obukhov profile, i.e. neglecting the finite extent of the source. In unstable stratification, due to the rapid deepening of the plume (and the "constant flux layer" at its base), the situation is very forgiving: indeed Fig. 2 shows that using the MO profiles will return an acceptable estimate provided the upwind end of the paths does not lie upwind of the leading edge (of course, outcomes depend in detail on the emitter and reflector heights z_c, z_u, z_d). In neutral stratification greater caution is needed with placement of the paths relative to the edge of the source, if one were to invert using the Monin–Obukhov profile; while in stable stratification it seems essential, for likely configurations of the detectors, that one would have to invert taking account of the fetch. Fig. 3 differs from Fig. 2 only in that the pathlengths have been doubled. As a result, when the measurement paths originate upwind from the leading edge of the source the error of neglecting the finite fetch of source in interpreting (inverting) ΔC to get Q, while still serious, is not *so* large as it had been with the shorter paths.

---

[4] In fact, even with very large x_c the solutions fail to match perfectly with Φ_{MO}, presumably because the power law profiles can match the MO profiles at only a single height H, the chosen reference height (this is not evident from the diagram). The choice $H = 1$ m made here is arbitrary, and any other choice would be equally so.
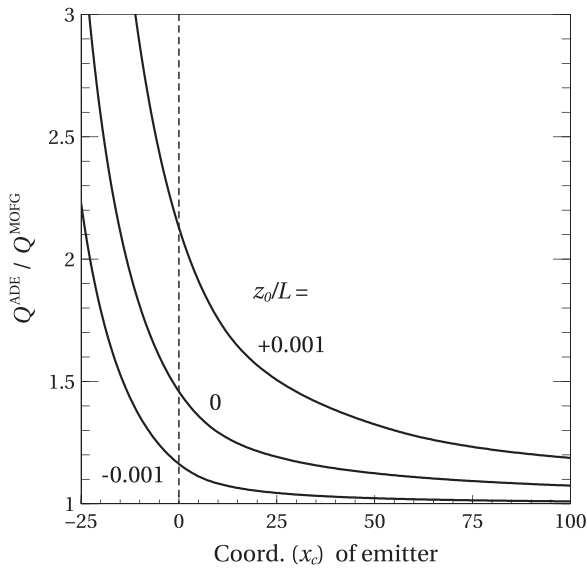
Fig. 4. Ratio Q^{ADE}/Q^{MOFG} of the emission rates that would be inferred by inverse dispersion based on the advection-diffusion equation (Q^{ADE} computed using Wilson, 1982, 2015a solutions) and by interpreting the measured concentration difference as that of a standard Monin–Obukhov profile (Q^{MOFG}). The latter is based on the difference of MO concentrations, correctly integrated along the beams, but neglecting the finite extent of source. Detector path lengths are 50 m, and (as throughout the paper) the leading edge of the source is at $x = 0$.

Evident from Figs. 2 and 3 is that although the conversion numbers Φ as computed by the Kormann–Meixner (or equivalently, Philip) and Wilson solutions to the ADE differ by up to about 20% in some circumstances, nevertheless they are in *qualitative* agreement and collectively flag the seriousness of neglecting the implication of a limited fetch. A useful way to emphasize this is to focus on the error in the inferred flux that will arise if the finite extent of the source giving rise to the path-averaged concentration signals is neglected (Figs. 4 and 5). If we focus on the very practical configuration with the emitter/detector placed at $x_c = 0$ (edge of the source) then in the case where the pathlength is only 50 m Fig. (4) indicates that in neutral stratification an error of $\sim$50% should be expected (as a consequence of having neglected the fetch limitation). The case of unstable stratification is much more forgiving, and probably even more so than Fig. 4 indicates because the role of the along wind velocity fluctuation u', which for $L < 0$ acts to deepen the constant flux layer, is neglected in the present analysis. However in (strongly) stable stratification the error will exceed 100%. Increasing the pathlength to 100 m (Fig. 5) provides some advantage: now with an emitter at $x_c = 0$ the error in neutral stratification drops to $\sim$20%.

3.1. Other path configurations

In terms of the configuration of the detector paths, it is evident that the line-averaged concentration difference ΔC will be more strongly weighted at positions x where the paths have greater vertical separation. The configuration shown in Fig. 1 gives least weight to the portion of the paths that is farthest upwind, whereas for the reverse configuration (reflectors lying upwind of the common emitter/detector) the opposite is true. Fig. 6 confirms that this 'reverse' configuration is less favourable, in terms of the needed upstream fetch of source.

It is also of interest to compare the slant path configuration (resembling Fig. 1, with $D_{x1} = D_{x2} = 50$ m) with the case that the detector beams, while unchanged in terms of their horizontal extent, are configured *horizontally* so as to achieve a larger mean height difference $\bar{\Delta}z_P$. For the slant path configuration
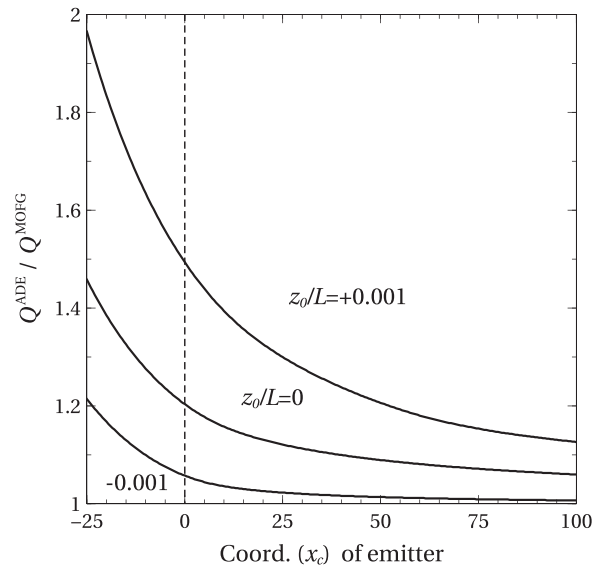

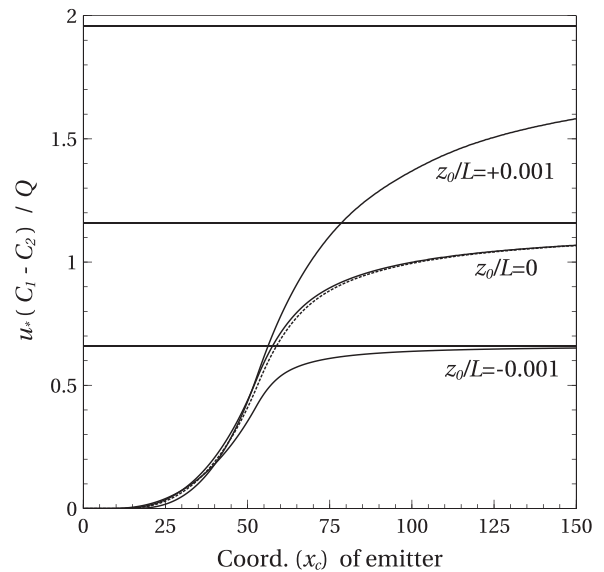**Fig. 5.** As for Fig. 4, except that here the averaging path length is 100 m.

Fig. 6. Solutions for the conversion number $\Phi = u_*(C_1 - C_2)/Q$ in the case that the reflectors are *upwind* from their common emitter/detector, and therefore nearer to the leading edge of the source (at $x = 0$). Horizontal lines are Φ_{MO}, and curves are Φ_W (Wilson, 1982, 2015a); the dotted curve is the neutral limit of the Wilson (2015a) solution with power law wind profile. The detector paths, both 50 m in along wind extent, slant down from $z_u = 2.5$ m and up from $z_d = 0.5$ m to $z_c = 1.5$ m, results being shown for the emitter/collector position ranging $0 \le x_c \le 150$ m. (Note: with $x_c = 0$ the detector paths lie entirely upwind of the leading edge.)

(underlying Fig. 2) one has $\bar{\Delta}z_P = 1$ m, while paired horizontal paths to/from the same reflectors at $z_r = (0.5, 2.5)$ m obviously yield $\bar{\Delta}z_P = 2$ m. Accordingly, and provided the (still, common) coordinate x_c of the two emitter/detectors is sufficiently far downstream from the leading edge of the source, the signal level $u_* \Delta C/Q$ is much larger with horizontal beams. However Fig. 7, covering only the neutral case and with Q^{ADE} evaluated using the Wilson (1982) solution, shows that the configuration with horizontal paths is less forgiving in regard to the necessary fetch x_c of source upwind from the emitter/detectors, because in this case there is equal weighting of the concentration difference $\bar{c}_1(x) - \bar{c}_2(x)$ all along the path $x_c \le x \le x_c + 50$ m. Provided x_c exceeds about 40 m, the penalty for neglecting the edge effect in the computation for Q is the same for both configurations, and smaller than 10%.
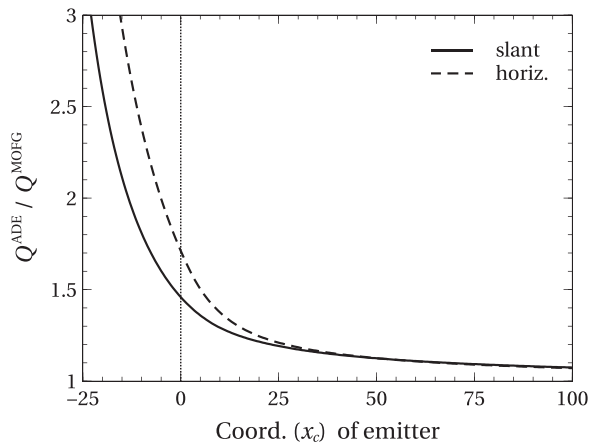
Fig. 7. Ratio Q^{ADE}/Q^{MOFG} of the emission rates that would be inferred in neutral stratification by inverse dispersion based on the advection-diffusion equation (Q^{ADE} computed using Wilson, 1982 solution) and by interpreting the measured concentration difference as that of a standard Monin–Obukhov profile (Q^{MOFG}). The detection paths span $x_c \le x \le x_c + 50\,m$ and results are shown with the emitter/detector coordinate ranging $-25 \le x_c \le 100\,m$. Two path configurations are compared: the slant paths, i.e. paths slanting up (or down) from $z_c = 1.5\,m$ to $z_u = 2.5\,m$ and $z_d = 0.5\,m$; and paired horizontal paths (the lower at 0.5 and the upper at 2.5 m) having the same projection onto the horizontal plane as do the slant paths.
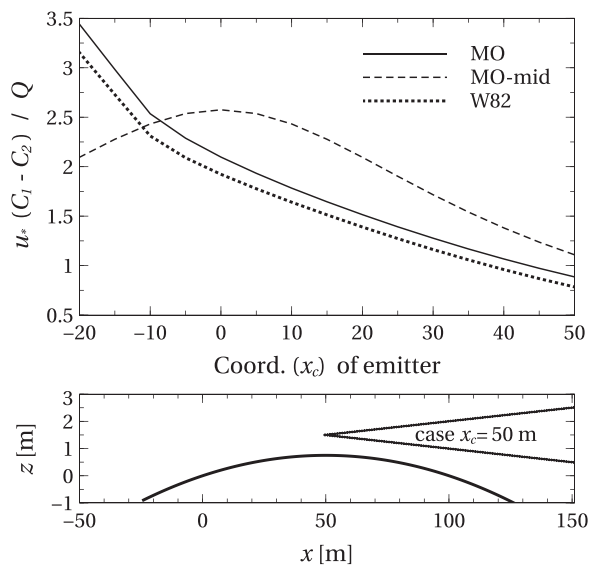

Fig. 8. Conversion number $\Phi = u_* \Delta C/Q$ for slant path flux-gradient measurements under neutral stratification over the topography shown in the lower panel, representing the detector beams as being *curved* so as to incorporate correctly their local height above ground. Φ is computed using either the Wilson (1982) concentration field (accounting for limited fetch) or the Monin–Obukhov profile (which assumes the fetch of source is infinite). The detection paths span $x_c \le x \le x_c + 100\,m$, slanting up (or down) from $z_c = 1.5\,m$ to $z_u = 2.5\,m$ and $z_d = 0.5\,m$, where the origin for these heights is ground level upwind from the terrain.

3.2. Influence of terrain

Fig. (8) is a simplistic view of the impact of a terrain feature on the inverse dispersion procedure, ground height $h = h(x)$ being specified as a gentle crosswind ridge. The path configuration is that of Fig. 1 with pathlengths $D_{x1} = D_{x2} = 100\,m$, $z_c = 1.5\,m$ and $(z_{r1}, z_{r2}) = (0.5, 2.5)\,m$ (these heights being measured relative to ground level upwind from the terrain bump). The calculation underlying Fig. 8 assumes the surface layer wind and turbulence fields are not perturbed by the terrain,

i.e. effectively this is an undisturbed surface layer in the terrain following coordinates $(x, z - h)$. Then the entire effect of the terrain is merely to perturb the effective height above ground of the detector beams, and the analysis is equivalent to the situation of *curved* detector paths over flat terrain (Hu et al., 2016 found that accommodating undulations of the ground in this manner does improve the performance of inverse dispersion using the backward Lagrangian stochastic model *WindTrax*). According to Fig. 8, if one were to invert to obtain the flux by adopting the MO profile (ignoring the fetch limitation), then one had best properly integrate the MO concentration difference along the beam (e.g. Eq. (24)), rather than difference the point concentrations at the beam midpoints.

4. Conclusion

The generalized flux-gradient (gFG) technique evaluated here exploits the capabilities of open path, line-averaging gas sensors. Based on the above findings and those of (Flesch et al., 2016) we recommend that if the fetch of source upwind of the concentration detectors limits depth of the constant flux layer, then the inversion (to get source strength Q from a mean concentration difference ΔC) should be done using a dispersion model that takes into account the source boundaries, and preferably without the approximations inherent in the analytical treatments surveyed above: in practise the backward Lagrangian stochastic (bLS) method is ideally suited, in every respect except its computational rapidity. At sites (and with source boundaries) compatible with their underlying assumption of crosswind symmetry, any of the Kormann–Meixner, Philip, or Wilson concentration fields could be adopted if it were desired to make a rapid, provisional estimate of the flux (with the proviso that the Philip solution does not apply to paths that cross the leading edge of the source). Simplest of all is to invoke the Monin–Obukhov concentration profile and compute the conversion number Φ_{MO}; if doing so, rather than evaluate the theoretical difference between concentrations at the two path midpoints it is preferable to integrate the concentration difference along the paired beams, using actual beam heights above the local terrain.

Should one choose to take the shortcut of neglecting the complications that an LS-based inversion entails (viz. mapping the source boundary, and carrying through what can be a time consuming calculation of the many needed ensembles of trajectories using, for instance, *WindTrax*), the results given here indicate that in unstable conditions (and to a lesser extent, neutral) the loss of accuracy is small for easily realizable configurations of the detectors: in reality, it is probably even smaller than we have indicated, owing to the impact of the along wind velocity fluctuation (u') and more importantly its correlation with the vertical velocity (Wilson, 2015b). Under stable stratification however there is no shortcut; if the fetch of source is "small" one will have to perform the inversion using one of the limited-fetch conversion numbers Φ (as above), or revert to the (more flexible and more rigorous) Lagrangian stochastic treatment.

Acknowledgements

References

Abramowitz, M., Stegun, I.A., 1953. Handbook of Mathematical Functions. Cambridge University Press.

Dyer, A.J., 1974. A review of flux-profile relationships. Boundary-Layer Meteorol. 7, 363–372.

Dyer, A.J., Hicks, B.B., 1970. Flux-gradient relationships in the constant flux layer. Q.J.R. Meteorol. Soc. 96, 715–721.

Flesch, T.K., Baron, V.S., Wilson, J.D., Griffith, D.W.T., Basarab, J.A., Carlson, P.J. Agricultural emissions during the spring thaw: applying a new measurement technique. Agric. For. Meteorol., 2016, (in press).

Hu, N., Flesch, T.K., Wilson, J.D. and Baron, V.S. Refining an inverse dispersion method to quantify gas sources on rolling terrain. Agric. For. Meteorol., 2016, (in press).

Kormann, R., Meixner, F.X., 2001. An analytical footprint model for non-neutral stratification. Boundary-Layer Meteorol. 99, 207–224.

Monin, A.S., Yaglom, A.M., 1977. Statistical Fluid Mechanics. MIT Press, pp. 769.

Philip, J.R., 1959. The theory of local advection. J. Meteorol. 16, 535–547.

Shwetz, M., 1949. On the approximate solution of some boundary layer problems. Appl. Math. Mech. 13 (3), 257–266 (in Russian).

van Ulden, A.P., 1978. Simple estimates for vertical diffusion from sources near the ground. Atmos. Environ. 12, 2125–2129.

Wilson, J.D., 1982. An approximate analytical solution to the diffusion equation for short-range dispersion from a continuous ground-level source. Boundary-Layer Meteorol. 23, 85–103.

Wilson, J.D., 2015a. Dispersion from a surface source in the unstable surface layer: an approximate analytical solution. Q.J.R. Meteorol. Soc. 141, 3285–3296, http://dx.doi.org/10.1002/qj.2609.

Wilson, J.D., 2015b. Computing the flux footprint. Boundary-Layer Meteorol. 156, 1–14, http://dx.doi.org/10.1007/s10546-015-0017-9.

Wilson, J.D., Flesch, T.K., Crenna, B.P., 2012. Estimating surface-air gas fluxes by inverse dispersion using a backward Lagrangian stochastic trajectory model. In: Lagrangian Models Atmosphere., pp. 149–161, American Geophysical Union, Geophysical Monograph 200 (349 pp.).